

Chapter - II

Preparation of Ferrites and
X-Ray Diffraction

2.1 INTRODUCTION :

The usefulness of ferrites is determined by their physical and chemical properties which fall in two categories, one being intrinsic to the constitution of ferrites and the other extrinsic i.e. structure sensitive. To the extent the method of preparation needs heat treatment for the formation of the crystal structure of the material, and also it influences the intrinsic properties which usually are to be understood in terms of cation distribution. However, the details of the heat treatment like firing temperature and time, atmosphere and cooling rate etc, cumulatively constitute the thermal history of the sample through the imprint on almost all the attendant micro-structural factors like grain size, defect concentration, porosity inclusions and orientation, size and shape of the grains.

The ceramic process make it possible to prepare complex chemical composition, desired microstructures and shapes of the final product much more economically, than the single crystals. Ceramics have sufficient mechanical strength to allow it to be formed in desired shape and machined according to application. Ceramics provide a way of avoiding undesired effects such as eddy current losses which can be suppressed by internal lamination along grain boundaries.⁽¹⁾

In this chapter a brief review of methods of preparation, ceramic process etc. are given. The method of preparation of ferrite samples in the laboratory is also briefly dealt with.

SECTION (A)

2.2 PREPARATION OF FERRITES :

Ferrites being the oxide materials no special extraction or preparation techniques involving molten phases are required. In the preparation, the starting materials are allowed to undergo solid state reaction and therefore, it is usually called ceramic process. Basically there are four steps in the preparation of ferrite materials for required applications. 1) Preparation of material to form an intimate mixture with the metal in the required ratio for final product .

- 2) Presintering or calcination.
- 3) Powdering of presintered material and pressing or forming the required shape.
- 4) Sintering to form the final ~~the~~ final product.

2.3 PREPARATION OF FERRITE COMPOSITION :

The general methods for preparation of ferrite compositions are given as follows :

- a) Oxide method
- b) Decomposition method
- c) Hydroxide method
- d) Oxalate method

2.3(a) OXIDE METHOD

This is most extensively used in the commercial production of ferrites, which requires little chemical knowledge. High purity of oxides of metals in the required proportion for final product are mixed together. One can mix carbonates with iron oxide. They are mixed manually and wet milled with steel balls for few hours. After milling, the mixture is dried, then the powder is passed through the mesh screen. The mixture is calcinated at elevated temperature and powdered and dried. Then pressed it into suitable shape and finally sintered.

2.3(b) DECOMPOSITION METHOD :

One may start with salts as carbonates, nitrates and oxalates instead of using oxides as starting materials. They are mixed in requisite proportion and preheated usually in air, produces oxides by thermal decomposition. The oxides

prepared 'in situ' are more readily undergo solid state reaction. ⁽²⁾ Other details of this method are similar to oxide method.

2.3 (c) HYDROXIDE PRECIPITATION :

Attempts have been made to precipitate simultaneously the required hydroxides from a solution to avoid lengthy milling process involved in dry mixing. The precipitate contains required metal ions in correct proportion already intimately mixed. Knowledge of solubility products of the substance is essential in order to determine the pH value of complete precipitation. Economos ⁽³⁾ established this method for the preparation of ferrites. Hydroxide precipitation method is also applied for preparation of YIG. ⁽⁴⁾ chemical process must be understood quantitatively in order to ensure the simultaneous precipitation of the hydroxides. If the simultaneity is not achieved the value of the method is lost. One or both of the precipitates may form in a state which may make filtration difficult. Sodium ions may be adsorbed on the precipitate getting occluded as impurities. ⁽⁵⁾ Sato and his ⁽⁶⁾ coworker prepared ultrafine spinel ferrites by this method and studied their properties .

2.3 (d) OXALATE PRECIPITATION :

Precipitation of metallic oxalates is preferable for some reasons. Precipitation can be carried out by using

ammonium oxalate which does not leave any residue after heating. Most metal oxalates are very similar in crystal structure. Therefore precipitation tends to produce mixed crystals which contain the metallic cations with correct proportions in which they were present in solution. Thus the mixing with correct ratio can be achieved on a molecular scale. ⁽³⁾ If the precipitation occurs, are widely different rates, mixed crystals do not form uniformly. Careful calcination at temperature of the precipitation yields ferrite with particle size less than $1 \mu\text{m}$.

2.4 PRESINTERING :

The purpose of the presintering is to decompose higher oxides and carbonates which reduces the evolution of gas in the final sintering process. Secondly it assists in homogenising of the material and also reduce the variations in the compositions of raw material. Lastly it is necessary to control the shrinkage of the material which occurs during final sintering. During the presintering the raw materials partly react to form final product and the amount of reaction depends on the reactivity of the components and on the presintering temperature. ⁽⁷⁾

2.5 SINTERING

The final microstructure develops during this sintering process. We assume that the cations are present in correct

proportions, the object then remains to achieve a suitable microstructure together with correct oxygen content and the distribution of cations. These are affected by the time and temperature of sintering, the partial pressure of oxygen or any other sintering atmosphere and cooling rate.

Sintering consists of heating the compact to a temperature at which the mobility is sufficient to permit the decrease of free energy associated with grain boundaries. Extensive reviews on grain growth and sintering are available. (8,9) During sintering densification and grain growth occur at the same time and give rise to a variety of microstructures. Sintering reactivity is important for densification.

This reactivity is defined as the amount of energy available for sintering must be sufficiently high for the process to proceed i.e. the particle size of the powder must be small. Surface energy is defined by an equation...

$$E = \frac{\sigma \pi D^2}{D} \dots\dots (2.1)$$

Where σ = Surface tension

D = Diameter of spherical powder particle.

As sintering and densification ^{for} require material to be transported, it is equally important that material possesses good sinterability, Volume diffusion is main transport

mechanism in ionic solids such as spinels . Surface diffusion may play a part in the beginning of the process in the formation of contact area between particles.

Before the start, the powder is compacted in such a way that the density is high to have good contact between particles. Nabarro⁽¹⁰⁾ Heiring⁽¹¹⁾ theory for diffusional microcreep is considered to be principle mechanism for densification. The surface of the pore act as source of vacancies. These vacancies diffuse through the bulk of the particles to the grain boundries, where they can be discharged. The resulting effect is material transport by the migration of individual ions from the grain boundries to the pores, producing shrinkage.

The sintering process is a sort of solid state reaction, consists of heating of the compacted material at temperature upto 1350°C, At this temp, mobility is sufficient to permit the decrease of the free energy associated with the grain boundries. The final microstructure together with the oxygen content and the distribution of the cations are greatly affected by time and temperature of sintering, the partial pressure of oxygen or any other sintering atmosphere and the cooling rate.

During the course of sintering densification and growth occurs simltenously. The grain growth mechanism during the

process of sintering is an interesting mechanism. Extensive reviews on grain growth and sintering are available.

2.6 SINTERING ATMOSPHERE :

It has been observed that sintering atmosphere plays an important role in sintering process. It must be remembered that Fe_2O_3 content can depend on the degree of oxidation or reduction of ferrite. Deficiency of Fe_2O_3 appears to lead to the highest eventual density for Ni-Zn ferrite but introduces second phase inclusions, It is fortunate that with the second phase inclusions, it is possible ^{near} to achieve 100% density at or very near to stoichiometric composition.⁽¹²⁾ The reduction of ferric to ferrous ion occurs at high temperature or at low oxygen pressure. The explanation for an effect of deficit Fe_2O_3 was given by Reigen.⁽¹³⁾

2.7 PREPARATION OF FERRITE SAMPLES :

2.7 (a) GENERAL FORMULA :

The ferrite samples are prepared usual ceramic method, starting with oxides. The general formula of the ferrite samples is ...

$$Cu_x Co_{1-x} Fe_2O_4$$

where
~~where~~ $x = 0, 0.2, 0.4, 0.6, 0.8, 1$

2.7 (b) METHODS OF PREPARATION : 2

The AR grade oxides CuO, CoO and $\alpha\text{-Fe}_2\text{O}_3$ were used for preparation which supplied by Riddle Heiag seize Honouer Germany. The oxides were weighed in required mole proportions on a single pan microbalance of least count 10^{-5} gm and mixed thoroughly in an agate-mortar with acitone. This mixture was dried in an oven at temperature 100°C . The dry mixture was then transferred into a platinum crucible and heated at 700°C for ten hours in a glowbar furnace. Afterwards temperature was slowly increased to 950°C and kept at that temperature for ten hours. Then the samples were furnace cooled by switching OFF the furnace. The temperature of furnace was measured with the help of chromel-Alumel thermocouple on D.R. potentiometer. The thin wires of cromel and Alumel were taken and fused one end and calibrated by usual method before measuring the temperature of the furnace. Thus presintered sample was taken out from the crucible. This hard sample was then ground in a ball mill with alcohol medium for four hours and dried at 100°C . Finally powder was collected in a clean dish.

2.7 (c) PELLET FORMATION :

Few grams of the sample was taken into agate mortar and wet mixture was done using P.V.A. as binder. Acitone was allowed to evaporate till the powder becomes completely dry. Then the dry powder was poured into die having 1cm diameter and cold pressed in a hydraulic press with the pressure of about 12-15 tonnes and load was left for 10 to 15 minutes.

After removing the load pellet was taken out from the die.

2.7(d) FINAL_SINTERING :

The pellets thus prepared were taken clean platinum foil and kept in glowbar furnace and sintered at 950°C for about 40 hours which is reported and judged to be the sufficient period for the completion of solid state reaction. They were then furnace cooled. The rate of cooling of the furnace was nearly 100°C/hour for first 2-3 hours and nearly 50°C/hour for the intermediate stage dropping to very low value asymptotically as the room temperature was approached with in a span of about 24 hours.

For X-ray diffraction studies, the pellets were again ground in a ball mill and the powder that was obtained was sieved through a mesh of 38 μ m. This gave a fine powder. Some pellet were reserved for use in resistivity and magnetisation measurement.

SECTION (B)

X-RAY_DIFFRACTION_STUDY

2.8 INTRODUCTION :

X-ray diffraction technique is ⁹ ~~an estimated and~~ well established tool for the study of the crystal structure. The details of X-ray diffraction study in short has been presented

in the next section. In order to confirm the crystal structure of ferrites and for determination of lattice parameter of spinel structure, we have been carried out X-ray diffraction studies of the series of $Cu_x Co_{1-x} Fe_2 O_4$ Ferrite.

2.9 CONDITION FOR X-RAY DIFFRACTION :

The regular three dimensional arrangement of unit cells in the crystals can be regarded as three dimensional diffraction grating for X-rays. According to Bragg⁽¹⁴⁾ diffraction, it is possible only when the wave length of X-rays is comparable with inter planer distance. The Bragg's law is

$$n\lambda = 2d \sin\theta \quad \dots\dots\dots (2.2)$$

Where d is the inter planer distance.

n is the integral number.

$$\theta < \sin\theta < 1 \Rightarrow n\lambda < 2d \quad \dots(2.3)$$

Since, $n = 1$ is the least value of n in the diffraction condition for any observable angle 2θ

$$n\lambda < 2d \quad \dots\dots\dots (2.4)$$

Bragg's law can be rearranged as

$$\lambda = \frac{2d}{n} \sin\theta \quad \dots\dots\dots (2.5)$$

Then coefficient of λ being unity, reflection of any order can be conveniently considered as the first order reflection

from planes real or imaginary, spaced at a distance $\frac{1}{n}$ of the previous spacing. For convenience, replacing $\frac{d'}{n}$ by d , we get

$$\lambda = 2d \sin\theta \quad \dots\dots\dots (2.6)$$

The applicability of the law can be illustrated from Fig.(2.1). The number of whole wavelengths lying in the path difference between rays scattered by adjacent (hkl) plane is known as the order of diffracted beam. Fig.(2.1a) represents the 2nd order (100) reflection. If there is no real plane midway between the (100) planes, it can be imagined as in Fig.2.1b forming 1st order reflection for adjacent (200) planes.

In the same way (300),(400) etc. reflections may be equivalent to the 3rd,4th etc. order from the (100) planes. Thus the 4th order reflection from (hkl) planes of spacing 'd' may be viewed as a first order reflection from (nh,nk, nl) planes of spacing $d = \frac{d'}{n}$. This suits with the definition of miller indices of planes parallel to the (hkl) planes with $\frac{1}{n}$ spacing of the latter.

The number of diffraction directions $2\theta_1, 2\theta_2, 2\theta_3$ etc.can be traced and photographed from the (100) planes by using a monochromatic incident beam at the angle $\theta_1, \theta_2, \theta_3$ etc. which produce first, second,third etc. order reflections. The diffraction from the other planes is also expected. The combination of Bragg's law and the plane spacing expression of a particular crystal under investigation predict the

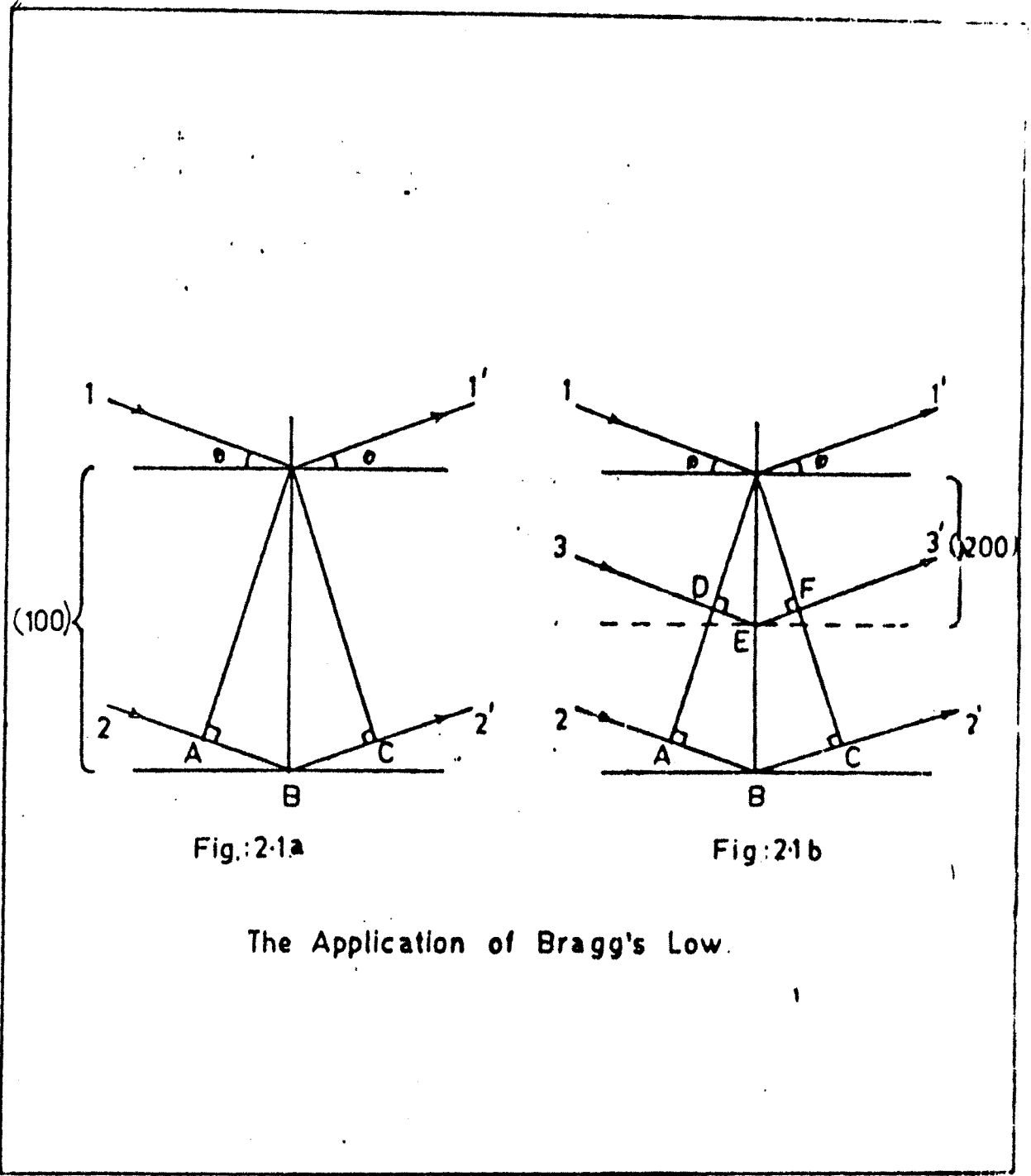


Fig. 2-1

diffraction angles for any set of planes.

For the cubic crystal,⁽¹⁵⁾ the interplanar distance in (hkl) set of plane is

$$\frac{1}{d^2} = \frac{h^2 + k^2 + l^2}{a^2} \dots\dots\dots (2.7)$$

Where 'a' denotes the unit cell size. Combining with the Bragg's law, we have

$$\sin^2 \theta_{hkl} = \frac{\lambda^2}{4a^2} (h^2 + k^2 + l^2) \dots\dots (2.8)$$

The equation becomes representative of Bragg angles for diffraction occurring from the plane (hkl) for known value of λ .

For tetragonal crystal⁽¹⁵⁾

$$\sin^2 \theta_{hkl} = \frac{\lambda^2}{4} \left(\frac{h^2}{a^2} + \frac{k^2}{a^2} + \frac{l^2}{c^2} \right) \dots\dots\dots (2.9)$$

Where a and c are axes of tetragonal.

Thus the diffraction direction as predicted by equations (2.8) and (2.9) are determined solely by the shape and size of the unit cell. The converse of this statement is most important as far as the crystal analysis is concerned. The measurements of directions of diffracted beam speculated the shape and size of crystal unit cell while their intensities gives the information regarding the positions of atoms. For the structural analysis of crystal, from the

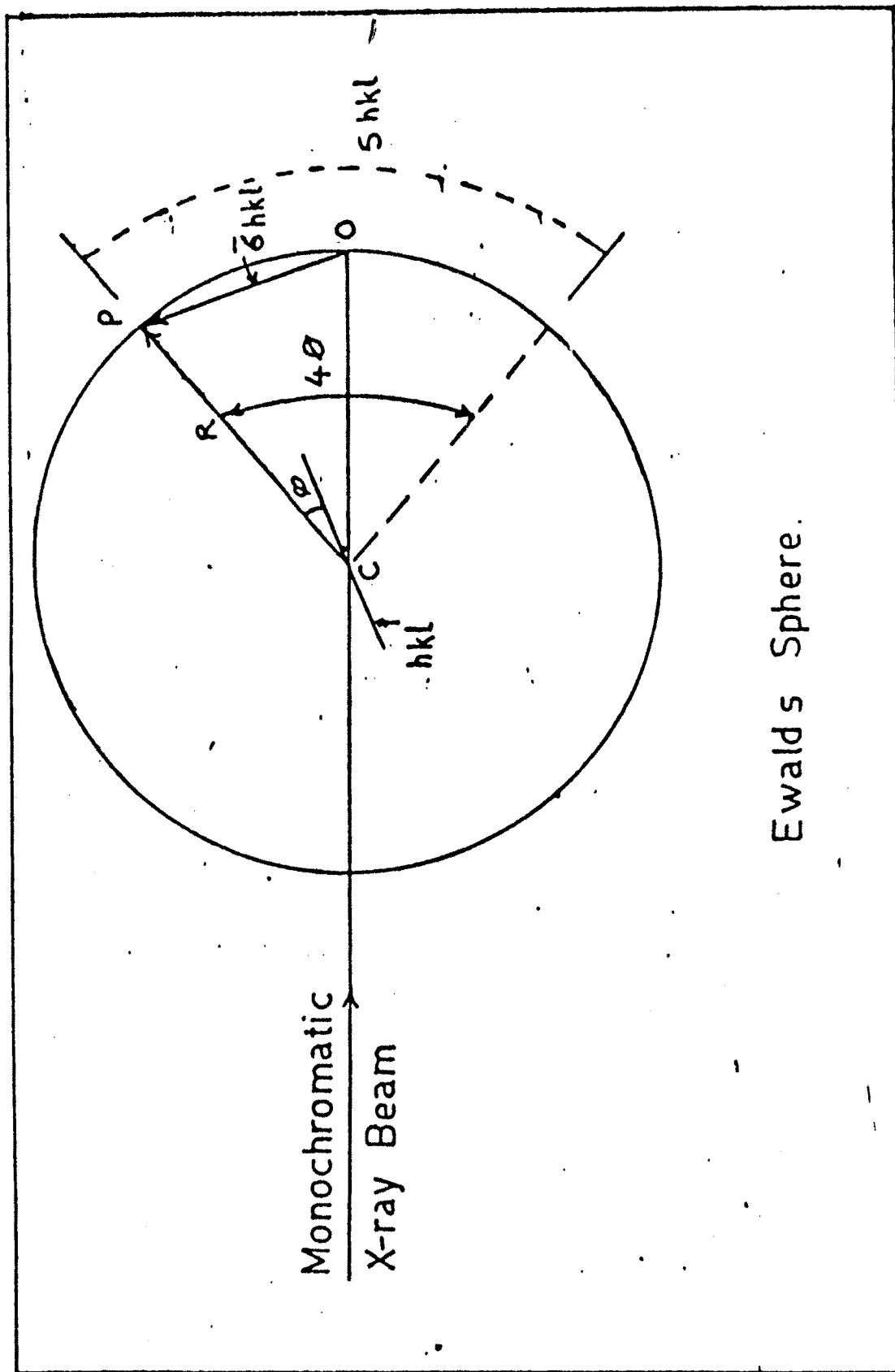
diffraction pattern, diffracted angles θ can be measured. For the known value of wavelength λ of x-rays used, inter planer distance d can be calculated by Bragg's law $\lambda = 2d \sin\theta$

2.10 POWDER METHOD AND ITS PRINCIPLE :

The powder method of x-ray diffraction was first developed by P. Debye and P. Scherrer⁽¹⁸⁾ in 1916 and independent by A.W. Hull⁽¹⁹⁾ in 1917. This method can be used properly to get the knowledge of structural information about the sample under investigation.

In this method the film is placed on the cylindrical surface of D.S. camera and the specimen holder rotates about the axis of the camera in a mono-chromatic beam of x-rays. The small amount of smoothly ground powder can be coated on the surface of a fine glass fiber with a glue or petroleum jelly. The specimen prepared is then mounted in its holder by proper adjustments.

The crystallites in a powder get completely randomly oriented so that the reciprocal lattice vectors of all the crystallites point in all the directions. The reciprocal lattice points lie on the surface of sphere of radii (hkl) . Each reciprocal lattice sphere oriented by every possible values of hkl cuts the Ewald's sphere Fig (2.2). A narrow film strip (plate A) is used to record the representative portion of the cuts.



Ewald's Sphere.

F. 5. 2. 2

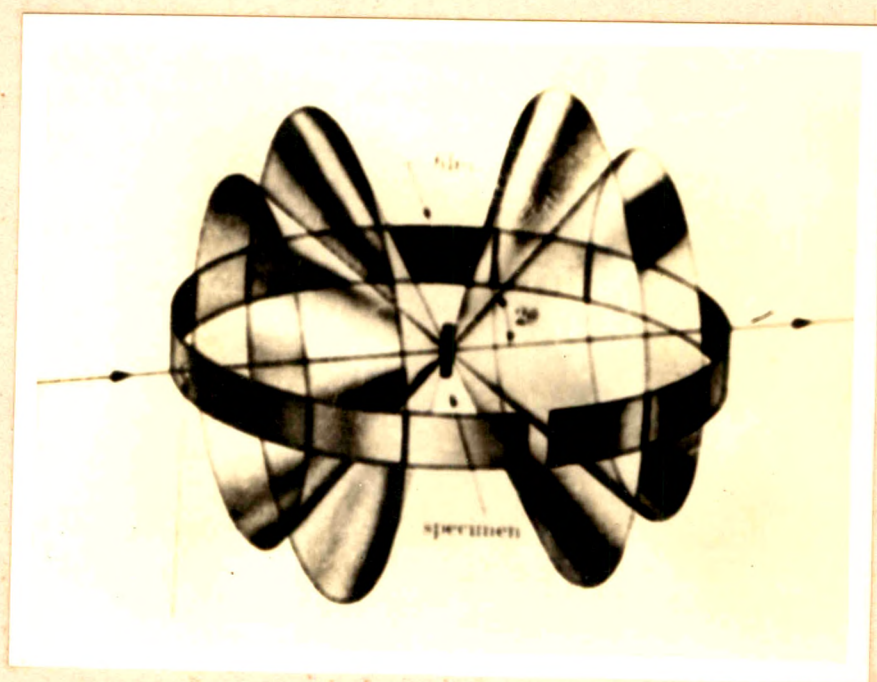


(plate A')

By the geometry of E Wald's sphere.

$$4 \theta_{hkl} = \frac{S_{hkl}}{R}$$

If we consider the two consecutive reflections, the angle between them is the Bragg angle which can be readily written as.

$$\theta_{hkl} = \frac{S_{hkl}}{4}$$

The measurements of S_{hkl} in mm on photographic film give the values of θ_{hkl} .

Using Bragg's law

$$2 d_{hkl} \sin \theta_{hkl} = \lambda \quad (2.10)$$

the interplaner distance d_{hkl} can be determined.

2.10 b) X-RAY DIFFRACTOMETER AND ITS PRINCIPLE :

The film in a Debye-Scherrer is replaced by a movable counter in an x-ray diffractometer.

The principle of the method and main features of the diffractometer are shown in Plate B'. The incident beam of x-ray free from K radiations made by use of a filter is allowed to pass through the slit (A') of the collimeter. The K radiations thus fall on the sample powder kept in a holder 'C' and get reflected by crystal planes satisfying the Bragg's law.

As the crystallites are randomly oriented, a reflection at the particular position is due to a set of atomic planes

which satisfy the Bragg's condition. The diffracted beam from the set of parallel planes of the specimen get converged and focused at a slit 'F' which further enters the counter 'G' with the help of special slit B, the diffracted beam is collimated. The counter 'G' is connected to a counter rate-meter. The output of the circuit is fed to Fast automatic recorder which registers the counts per second versus the angle ' 2θ '. The location of the centroid of the peak registered gives the values of $2\theta_{hkl}$ for the corresponding Bragg's reflection.

The carriage 'E' supports the receiving slits and the counter. The carriage 'E' is free to rotate about an axis 'C'. The angular position ' 2θ ' of the carriage and hence that of the counter G may be noted on the graduated circular scale 'K'. The mechanical coupling of 'E' and 'H' is made, so that the rotation of the counter G through an angle 2θ degrees moves the Specimen (C) through an angle θ degrees. It also ensures that the complementary angles of incidence and reflection from the flat specimen are always equal to each other, each being half the total angle of diffraction. This type of arrangement is necessary to satisfy the focusing conditions. The power driven counter moves with constant angular velocity about the axis of the diffractometer. For any desired angular range from 10° to 160° . The main advantage of the diffractometer over the Debye Scherrer powder method is that it gives a quantitative measure of the intensity.

2.11 EXPERIMENTAL :

The x-ray diffraction of ferrite system $\text{Cu}_x \text{Co}_{1-x} \text{Fe}_2 \text{O}_4$ (with $x=0.0, 0.2, 0.4, 0.6, 0.8, 1.0$) were taken by using Philips make P.W. 1051 P.M. 9920 x-ray diffractometer.

The samples of $\text{Cu}_x \text{Co}_{1-x} \text{Fe}_2 \text{O}_4$ were used in the fine powder form with the proper skill, powder could be mounted in the screens of sample holder so as to form plane surface of the specimen.

Co target was used. The wavelength of Co K_α being 1.7902 \AA .

The speed of chart was 1 degree per cm. rotation angle. The recording had been made from 20° to 80° of 2θ . The reflections were indexed by usual method.

2.12 INDEXING OF THE POWDER PATTERN :

The powder pattern of each slow cooled sample of the system $\text{Cu}_x \text{Co}_{1-x} \text{Fe}_2 \text{O}_4$ ($0 < x < 1$) were obtained with a diffractometer. The object of scanning was kept to cover as wide range of 2θ as possible between 20° and 80° . The value of $\sin 2\theta$ was calculated for each peak observed in the pattern. The set of these $\sin^2 \theta$ values is the raw material for the determination of cell size and shape.

For cubic lattice, the relation between the interplanar distance d_{hkl} , lattice parameter a , and the indices hkl can be represented by the formula⁽²⁰⁾

$$d_{hkl} = \frac{a}{\sqrt{h^2 + k^2 + l^2}} \quad \dots\dots(2.11)$$

As the peak in the diffraction pattern is obtained the Bragg's law must be obeyed,

$$2 d_{hkl} \sin \theta_{hkl} = \lambda \quad \dots\dots (2.12)$$

combining these two equations,

$$2 \left(\frac{a}{\sqrt{h^2 + k^2 + l^2}} \right) \sin \theta_{hkl} = \lambda$$

$$\therefore \frac{\sin^2 \theta_{hkl}}{h^2 + k^2 + l^2} = \frac{\sin^2 \theta_{hkl}}{S} = \frac{\lambda^2}{4a^2} \dots\dots(2.13)$$

Where the sum $S = h^2 + k^2 + l^2$

The sum S , is always an integer and the value of $\frac{\lambda^2}{4a^2}$ must be constant for any observed peak in the pattern. Thus the set of integers S should be selected properly to yield a constant quotient when divided one by one into the observed $\sin^2 \theta$ values. Rearranging the equation (2.13)

$$\sin^2 \theta_{hkl} = \frac{\lambda^2 S}{4a^2} \quad \dots\dots(2.14)$$

We find that the quantity $\frac{\lambda^2}{4a^2}$ is the greatest common factor (G C F) in $\sin^2 \theta$. As a first step GCF was determined from a

few lines at the lower angles and then all the other proper integers were found. Once the integers S were known, the indices hkl of reflecting plane were written down by inspection. When a set of integers satisfying equation (2.13) were not found, the other possible tetragonal system was checked and found in good agreement.

For a tetragonal unit cell⁽²⁰⁾ the relation can be written

$$d_{hkl} = \left(\frac{h^2 + k^2}{a^2} + \frac{l^2}{c^2} \right)^{-\frac{1}{2}} \dots\dots\dots(2.15)$$

Where 'a' and 'c' are the lattice parameters, combining this with Bragg's relation, we get,

$$\sin^2 \theta_{hkl} = \frac{\lambda^2}{4} \left(\frac{h^2 + k^2}{a^2} + \frac{l^2}{c^2} \right) \dots\dots\dots(2.16)$$

$$\text{Or } \sin^2 \theta_{hkl} = A (h^2 + k^2) + c.l^2 \dots\dots\dots(2.17)$$

$$\text{Where } A = \lambda^2/4a^2 \text{ and } c = \lambda^2/4c^2 \dots\dots\dots(2.18)$$

For crystals having tetragonal symmetry the patterns are more complicated. The simplest analytical method to index such a pattern is to find relationships between the values of $\sin \theta$ which yield an indication of the crystal symmetry. The value of the factor A was computed by using eq (2.18) for $l=0$.

The allowed values of $(h^2 + k^2)$ are 1,2,4,5,8 etc. Thus the hkl lines must have the values of $\sin \theta$ of the ratio of these integers. Where A will be some number 1, 1/2, 1/4, 1/5, 1/8, etc. times the values of $\sin \theta$ of these peaks in the pattern substituting the values of A in equation (2.17) for known values of $\sin \theta$ with $l = 1,2,3$ the factor c was determined. Making use of these common factors, all the reflections were indexed. The lattice parameter 'a' was obtained from the reflections for which $l = 0$ substituting this value of 'a' for reflections at higher angles, the value of 'c' was calculated.

2.13 RESULT AND DISCUSSIONS :

X-ray diffractometric records of slow cooled $\text{Cu}_x\text{Co}_{1-x}\text{Fe}_2\text{O}_4$ were obtained and shown in Figs.(2.3 a,b,c,d,) The diffraction maxima were indexed by G C F method as explained else where and were checked and tallied with those expected for spinel structure^(21,22)

The reflections for cubic structure are (111), (220), (311), (222), (400), (422), (333), (115) and (440) and for tetragonal structure the planes observed are (111) (202) (220) (113) (311) (222) (400) (004) (224) (422) (440) (404) .These planes are allowed for spinel structure. The d values of the

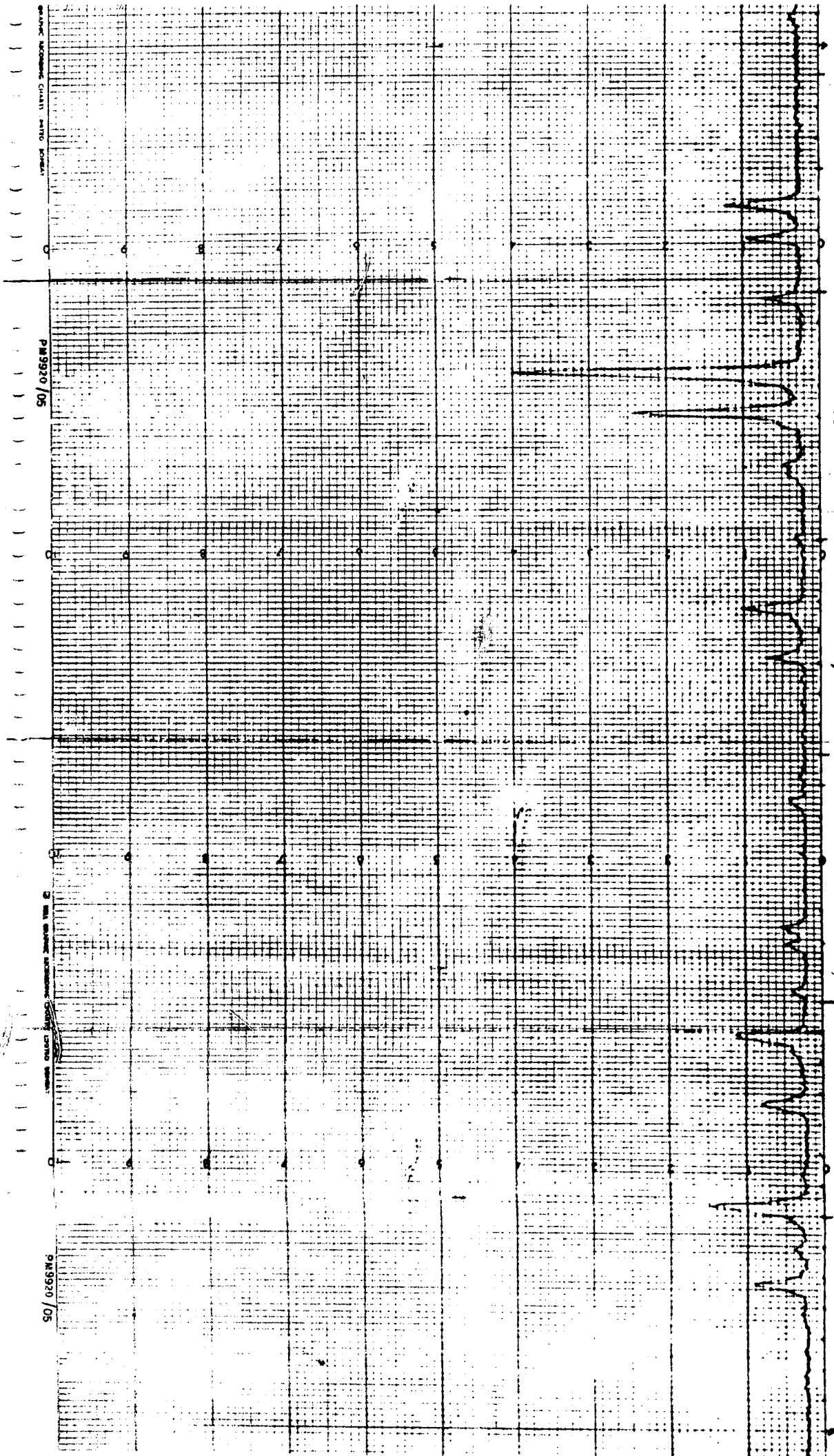


FIG. 2-3a

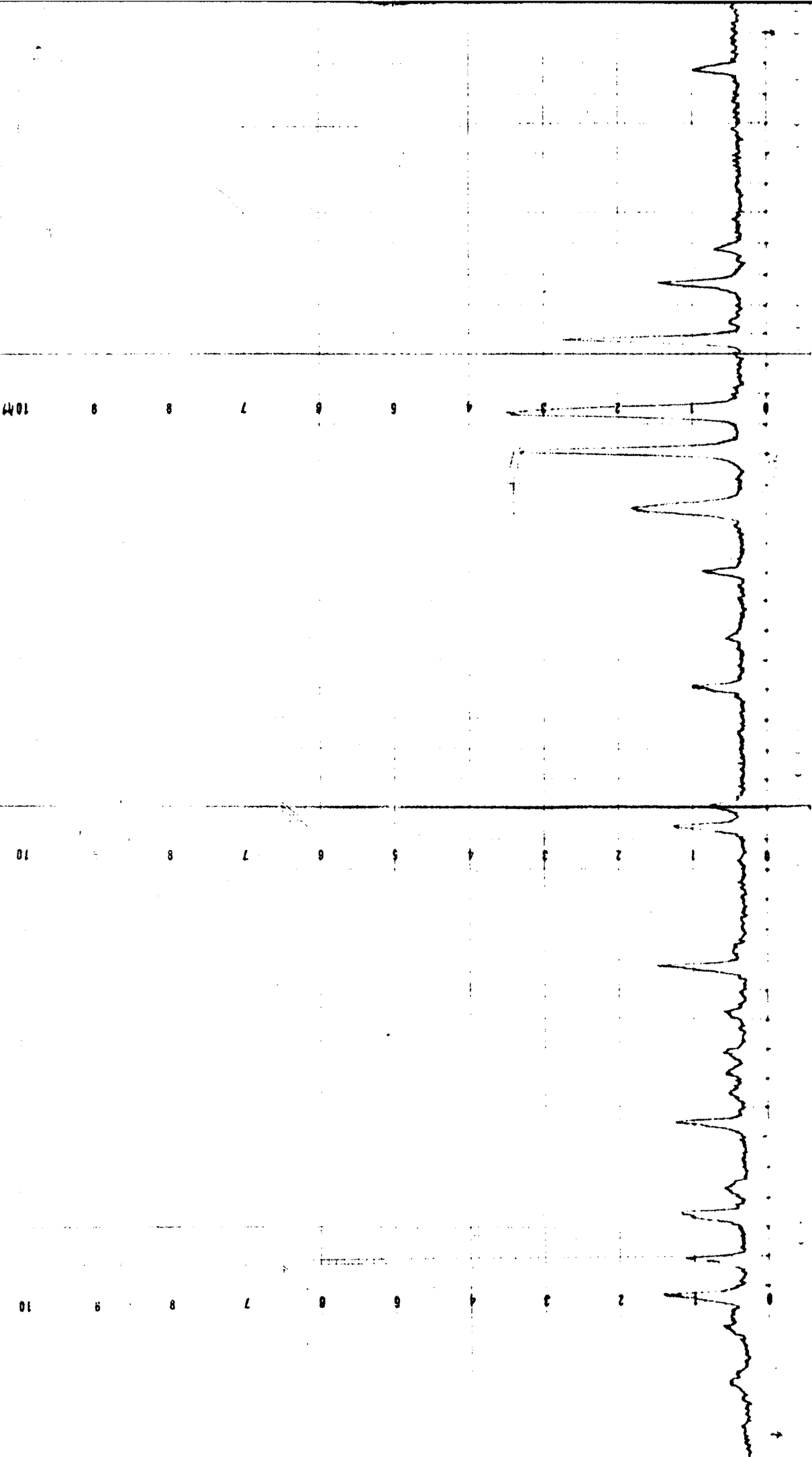


FIG. 2-3 b

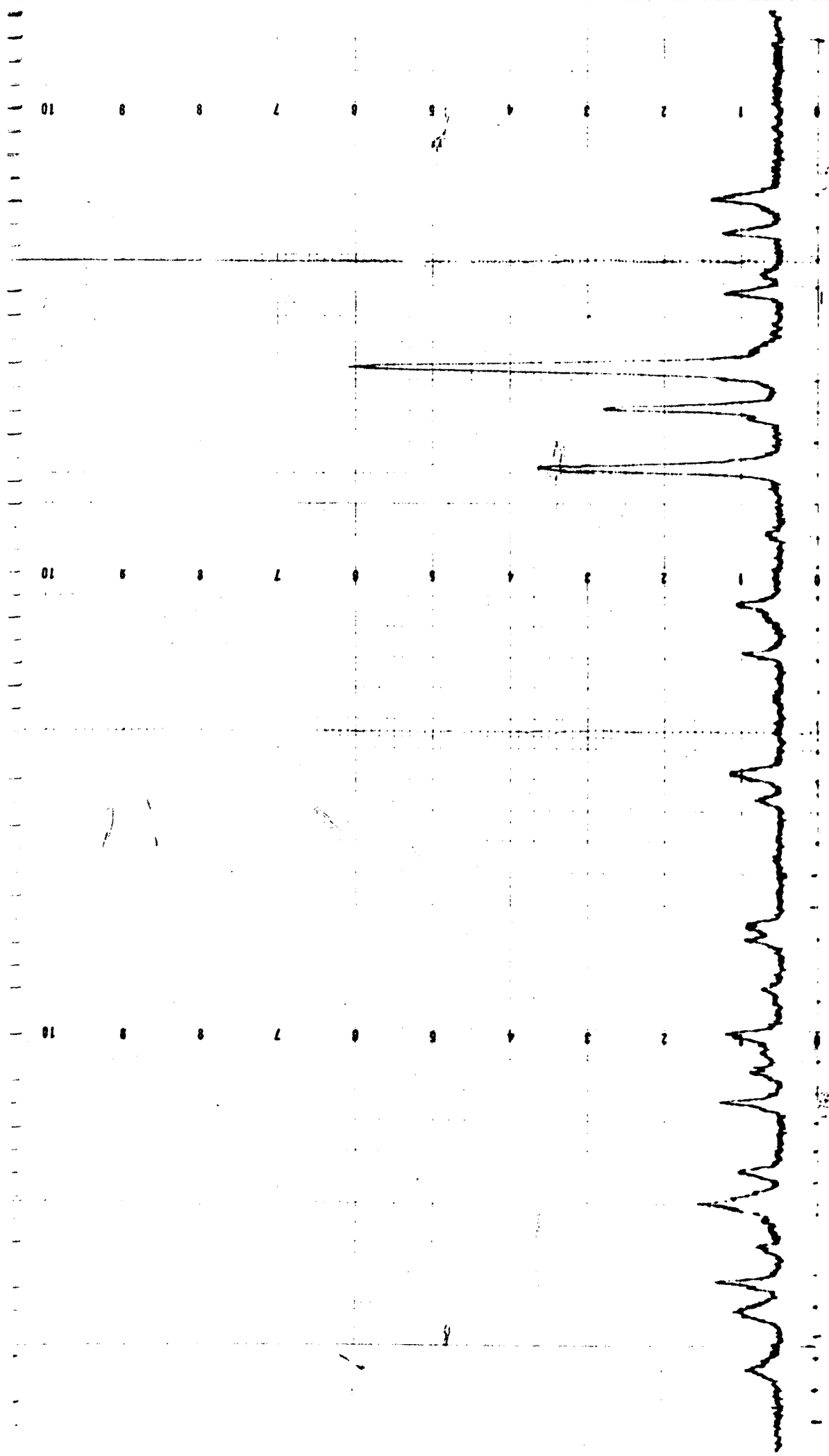


FIG. 2-3c

59

813 (2.3c)

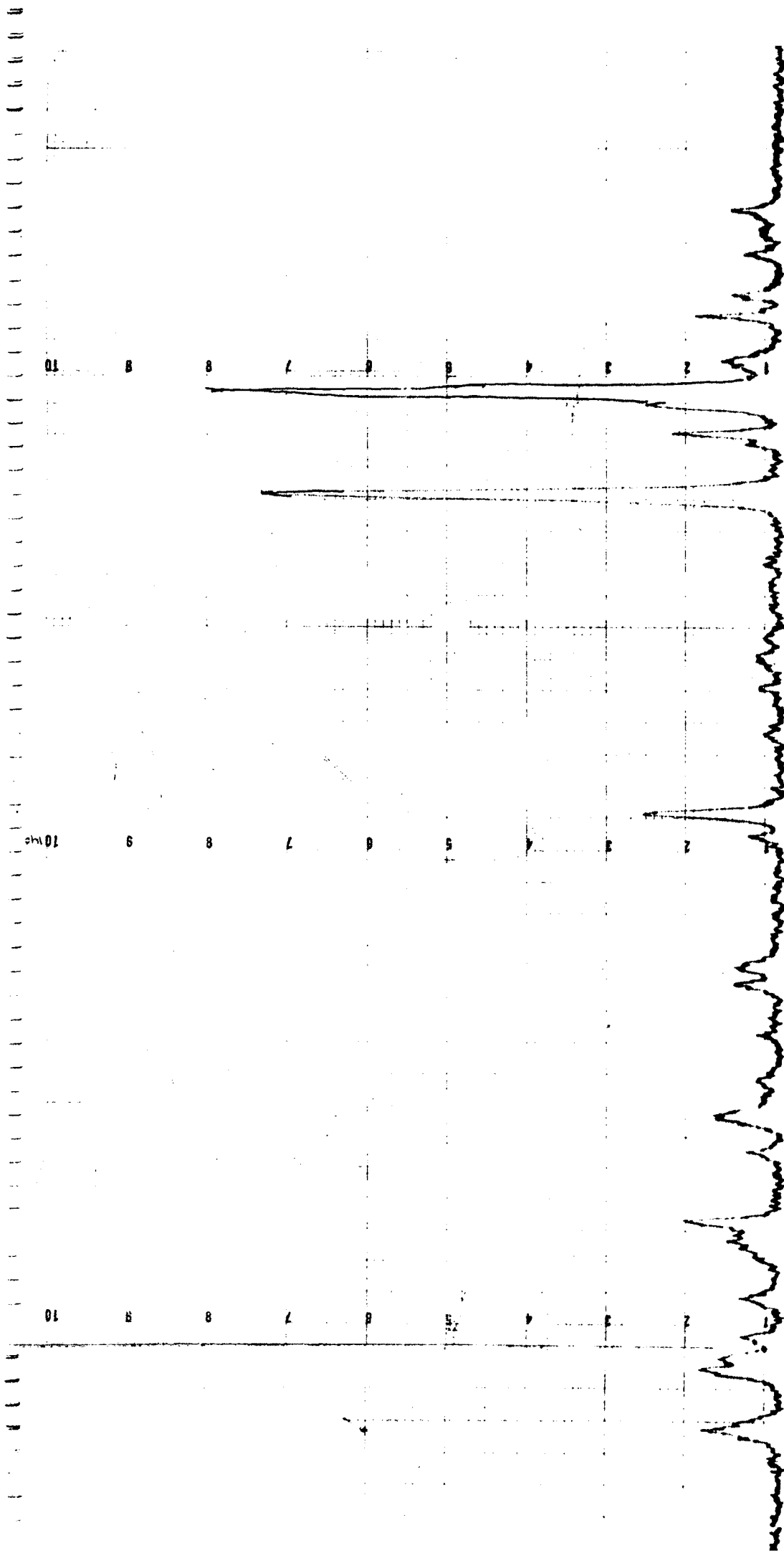


FIG. 23d

samples ($\text{Cu}_x \text{Co}_{1-x} \text{Fe}_2 \text{O}_4$) for ($x = 0.8, 0.6, 0.4, 0.2$) are represented in table Nos. (2.1, 2.2, 2.3, 2.4). The calculated d values of the samples are in close agreement with the observed d values, which clearly indicates the ferrites prepared are fully formed with spinel structure.

The lattice parameter a and c were determined for different compositions of the system. In table (2.5) the composition, x , lattice parameter $c, a, c/a$ and a^* are given.

It is observed the tetragonal ratio decreases with decrease Cu content in the system and becomes one. The tetragonal structure is observed $x = 1.0, 0.8, 0.6,$ and 0.4 and cubic structure for 0.2 and 0.0 .

Delorme (22) has examined the lattice distortion in $\text{Cu}_{1-x} \text{M}_x \text{Fe}_2 \text{O}_4$ where ($M = \text{Ni, Mg, Co}$) and also for $\text{Cu}_x \text{Zn}_{1-x} \text{Cr}_2 \text{O}_4$. Ohnishi and Ferenshi (23) have suggested that if one takes into the consideration the Delrone results along with the site preference energies almost all Cu ions must go on B site for ferrites and A site for chromites. According to site preference energies of Co^{+2} , the Co ion in ferrite should go to B site only. This clearly indicates as the decrease of Cu ion or increase of Co ion in this system the distortion decreases with increase of Co ion by replacing Cu ions at B site.

TABLE NO. 2.1

SAMPLE S₁ - Cu_{0.2} Co_{0.8} Fe₂O₄

Sr. No.	hkl planes	d Å ^o calculated	d Å ^o observed
1.	(220)	3.02	2.83
2.	(113)	2.63	2.70
3.	(222)	2.46	2.43
4.	(400)	2.13	2.13
5.	(313)	1.98	1.98
6.	(331)	1.96	1.96
7.	(404)	1.87	1.83
8.	(224)	1.80	1.78
9.	(422)	1.74	1.72
10.	(333)	1.65	1.65
11.	(440)	1.51	1.51
12.	(531)	1.46	1.46
13.	(206)	1.38	1.42

Lattice parameter a = 8.552 Å^o

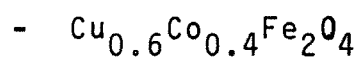
TABLE NO. 2.2.

Sample - $\text{Cu}_{0.4} \text{Co}_{0.6} \text{Fe}_2\text{O}_4$

Sr. No.	hkl plane	d A ^o calculated	d A ^o observed
1.	(111)	4.95	4.27
2.	(202)	3.03	2.92
3.	(220)	3.01	2.82
4.	(113)	2.60	2.68
5.	(311)	2.57	2.55
6.	(222)	2.47	2.34
7.	(004)	2.16	2.16
8.	(400)	2.13	2.13
9.	(331)	1.97	1.96
10.	(313)	1.95	1.92
11.	(224)	1.75	1.80
12.	(422)	1.74	1.74
13.	(115)	1.66	1.68
14.	(511)	1.64	1.65
15.	(404)	1.52	1.59
16.	(440)	1.50	1.51
17.	(531)	1.44	1.46

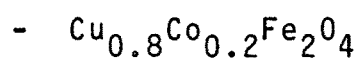
Lattice parameter a = 8.536 A^oc = 8.667 A^o

SAMPLE NO. 3



Sr. No.	hkl planes	d A ^o calculated	d A ^o observed
1.	(202)	3.03	2.93
2.	(220)	3.01	2.83
3.	(311)	2.60	2.68
4.	(113)	2.57	2.56
5.	(222)	2.47	2.44
6.	(004)	2.16	2.16
7.	(400)	2.13	2.13
8.	(313)	1.97	1.98
9.	(331)	1.96	1.97
10.	(224)	1.76	1.75
11.	(422)	1.74	1.71
12.	(115)	1.66	1.68
13.	(333)	1.65	1.66
14.	(511)	1.64	1.64
15.	(404)	1.52	1.59
16.	(440)	1.50	1.48
17.	(531)	1.46	1.46

Lattice parameter a = 8.535 A^oc = 8.654 A^o

TABLE NO. 2.4SAMPLE - S₄

Sr. No.	hkl planes	d A° calculated	d (A°) observed
1.	(111)	4.95	4.27
2.	(202)	3.04	2.92
3.	(220)	3.02	2.82
4.	(113)	2.70	2.69
5.	(222)	2.47	2.39
6.	(004)	2.16	2.16
7.	(400)	2.13	2.13
8.	(331)	1.96	1.96
9.	(224)	1.75	1.75
10.	(422)	1.74	1.69
11.	(115)	1.66	1.66
12.	(511)	1.64	1.64
13.	(333)	1.64	1.63
14.	(404)	1.52	1.59
15.	(440)	1.51	1.51
16.	(531)	1.44	1.46

Lattice parameter a = 8.552 A°

c = 8.650 A°



TABLE NO. 2.5

LATTICE PARAMETER AND TETRAGONALITY RATIO WITH COMPOSITION OF CU.

Sr. No.	Composition	Crystal structure	Lattice constant		c/a	$a^* = \sqrt{a^2 c}$
			$\frac{a}{\text{Å}}$	$\frac{c}{\text{Å}}$		
1.	CoFe_2O_4	C	8.38	-	1	8.375
2.	$\text{Cu}_{0.2}\text{Co}_{0.8}\text{Fe}_2\text{O}_4$	C	8.552	-	1	8.553
3.	$\text{Cu}_{0.4}\text{Co}_{0.6}\text{Fe}_2\text{O}_4$	T	8.536	8.667	1.014	8.578
4.	$\text{Cu}_{0.6}\text{Co}_{0.4}\text{Fe}_2\text{O}_4$	T	8.535	8.654	1.014	8.574
5.	$\text{Cu}_{0.8}\text{Co}_{0.2}\text{Fe}_2\text{O}_4$	T	8.552	8.650	1.015	8.584
6.	CuFe_2O_4	T	8.255	8.700	1.054	8.401

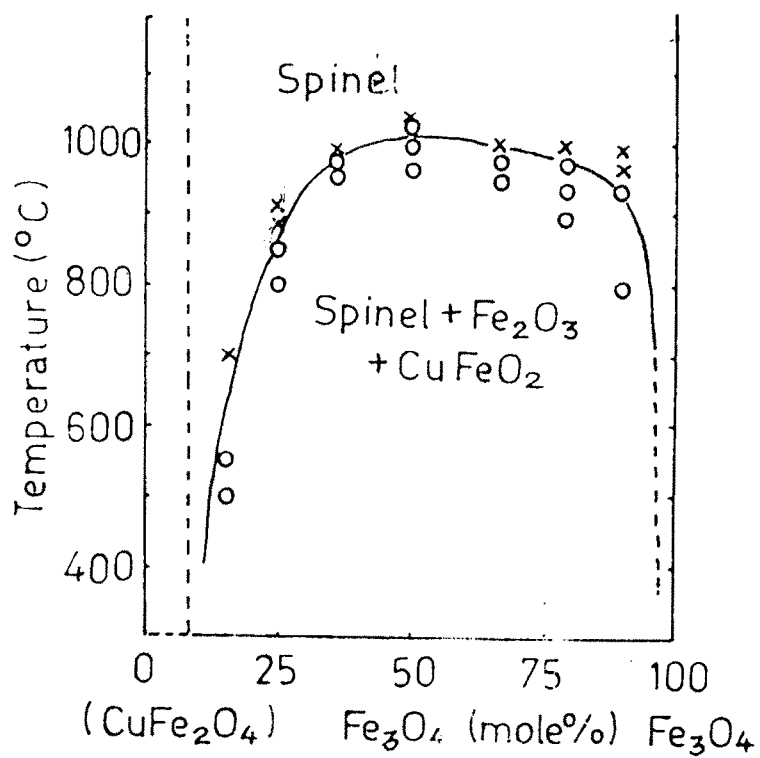
The phase relationship of Cu-Fe-O (fig 2.4) was suggested by Yamaguchi and Sirashi⁽²⁴⁾ They have observed the eutectoid decomposition of CuFe_2O_4 - Fe_3O_4 solid solution. Above 1005°C the spinel solid solution is stable through out the composition.

The eutectoid temperature was found to decrease with the addition of copper ferrite or magnetite. It is observed that most spinel solid solutions are unstable even under the non oxidising conditions and at low temperatures.

The phase relationship of Co-Fe-O was suggested by E.M; Levin et al⁽²⁵⁾ Apart from the⁽²⁶⁾ Fig (2.5) transformation at 900°C of Co_3O_4 in CoO several two phase regions are noticed. For compositions between CoFe_2O_4 and Co_3O_4 a two phase system (S+W) of spinel S and Wüstite is formed above a temperature that depends on Co-Fe ratio.

After firing such compounds in this two phase region one finds that upon cooling the second phase (W) will not necessarily disappear by dissolving into the spinel. The metastable wustite phase also contains some divalent iron.⁽²⁶⁾

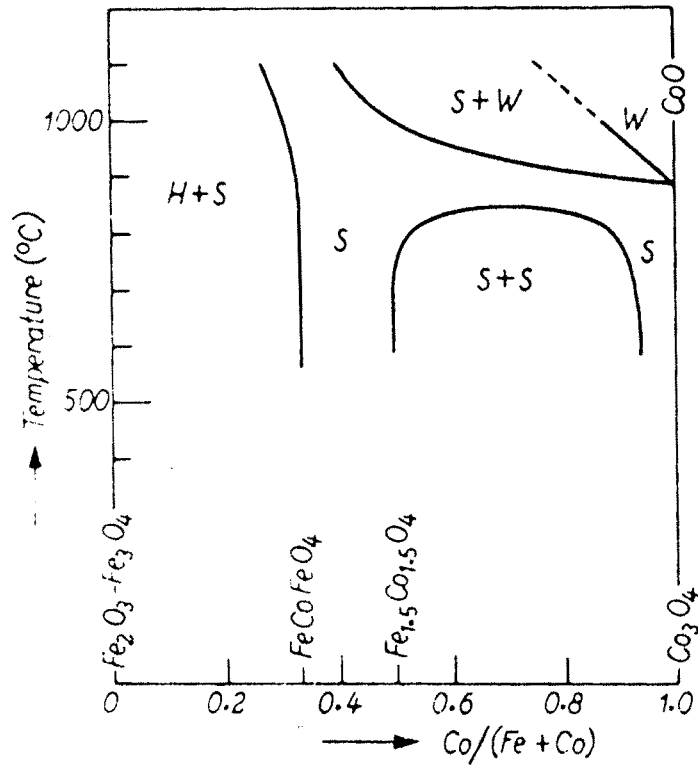
For $\text{Cu}_x\text{Co}_{1-x}\text{Fe}_2\text{O}_4$ the phase diagram is not known but the same difficulties may be expected. For our system, in x-ray diffraction patterns, some of the extra diffraction lines



Relation between eutectoid temperature & spinel composition. x: spinel; o: spinel + Fe₂O₃ + CuFeO₂

FIG. 2.4

Fig (2.5)



Phase diagram of the system CoO-FeO. S=Spinel, H=hematite ($x-Fe_2O_3$), W=wustite(FeO, CoO)

FIG. 2.5

have observed, which may be due to formation of Co_3O_4 or rFe_2O_3 or S+S solid solutions. According to Delome studies the lattice distortion vanishes at $X = 0.4$ for Co but in our system it shows $X = 0.6$ for Co. This variation may be due to temperature of preparation of ferrites and the phases which are involved during the preparation and preparation conditions. The preparation temperatures and oxidation conditions are different for Co and Cu ferrites.

R E F E R E N C E S :

1. E.Hirota, Jap.J.Appl. phys 5 1125 (1966).
2. K.J. Standley 'Oxide magnetic materials' chap.2 P.9
clearendon press New York (1972).
3. G.Economus J.Ame cera Soc.38 241 (1955).
4. W.P. Wolf, G.P. Rodrigue, J.Appl. phys.29 105 (1958).
5. T.Sato IEEE Trans Mag MAG 6 798 (1970).
6. T.Sato,C.Kuroda,M.Saito ferrites proc. Int conf Kyoto
Tokyo press P.72 (1970).
7. D.Swallow, A.K.Jordon,proc Brit ceram soc 2 1 (1964).
8. R.L. Coble,J.E. Burke,progress in ceramic Sci vol III
P.197 (1963).
9. A.L. Stuijts,C.Kooy,Sci ceram 2 231 (1965).
10. F.R.N.Naburro, Rept conf strength of solids phys Soc
London P 75 (1948).
11. C.Herring,J.Appl phys 21 2137(1950).
12. A.L. Stuijts proc Brit ceram soc 2 73 (1964).

13. P.J.L. Reigenen science of ceramics 4 169 (1968). 72
14. C. Kittel, 'Introduction to solid state physics' 5th Edn
John Wiley and sons INC NY (1976).
15. B.D. Cullity 'Element of x-ray diffraction' Addison
Wesley publishing co. INC. England (1959)
16. A. Taylor 'X-ray metallography' John Wiley and sons Inc
New York (1961).
17. C. Kittel 'Introduction to solid state physics' 3rd Edn
Wiley Eastern private Ltd, New Delhi.
18. P. Debye and P. Scherrer physick Z 17 277 (1916) and 18
219 (1917).
19. A.N. Hull phys. Rev. 9 84,564 (1916) and 10 661 (1917).
20. Henry, N.F.M. Lipson H. and Wooster W.A. The
interpretation of x-ray diffraction photographs.
Macmillan and Co. Ltd., London (1961).
21. Cullity B.D. Elements of x-ray diffractions addition
Wesley Pub. Co. Inc England (1959).
22. Delorme C, Thesis Grenoble (1956).

23. Ohinishi.H.Tereneshi T.
J.phys Soc Jap 16 35 (1961).
24. Yamaguchi T, Shiraishi T:
'Ferrites' Int conf on ferrites proc (Japan)
P.148 (1970).
25. Levin E.M. Robbins C.R. and Mcurdie H.F. phase
diagrams for ceramists AM cer soc (1964).
26. Broese van Groenou. A, Bongers P.F. stuyts A.L. Mat
Sci Eng 3 317 (1968/69).